

Cross-polarization OCT Assessment of Dentin Interface with Combinations of Adhesives and Composites

Turki A Bakhsh^{1*}, Halah M Alturkstani², Razan N Alharbi¹, Hind J Alrefai², Tahani O Badeeb², Nour H Altouki², Ahmed O Jamleh³ and Ehab N Alshouibi⁴

¹Department of Operative Dentistry, Faculty of Dentistry, King Abdulaziz University, Jeddah, Saudi Arabia

²Faculty of Dentistry, King Abdulaziz University, Jeddah, Saudi Arabia

³College of Dentistry, King Abdullah International Medical Research Center/King Saud bin Abdulaziz University for Health Sciences - National Guard Health Affairs, Riyadh, Saudi Arabia

⁴Department of Dental Public Health, Faculty of Dentistry, King Abdulaziz University, Jeddah, Saudi Arabia

***Corresponding Author:** Turki A Bakhsh, Department of Operative Dentistry, Faculty of Dentistry, King Abdulaziz University, Jeddah, Saudi Arabia.

Received: April 22, 2019; **Published:** May 15, 2019

Abstract

The current study aimed to compare the adaptation of two resin composite materials in restoring class-I cavities with two self-etch adhesive systems using cross-polarization optical coherence tomography (CP-OCT). Cylindrical class-I cavities were prepared on forty extracted human premolars. Two self-etch adhesives; Clearfil SE bond 2 (SE; Kuraray Noritake Dental, Japan) and Bond Force (Palfique Bond) adhesive (PL; Tokuyama Dental, Japan) were used in combination with two composites materials; Herculite XRV microhybrid dental composite (HRV; Kerr, Italy) and Estelite Alpha composite (ESA; Tokuyama Dental, Japan). The specimens were divided into four groups (n = 10); SE-HRV, SE-ESA, PL-HRV and PL-ESA. All specimens were submerged in a contrasting medium. After that, all groups were optically imaged under CP-OCT at every 250 µm interval distance. Then, image binarization and gap quantification were carried out using ImageJ analysis software. There was a statistically significant difference between all the groups except between SE-ESA and PL-ESA (p > 0.05). The highest median gap percentage was seen in PL-HRV group (56.15%) followed by SE-ESA (1.62%), PL-ESA (0%) and SE-HRV (0%), respectively. Other than composite filler loading and adhesive formula, the interactions of the adhesive and composite co-polymers might have a great influence on composite adaptation.

Keywords: Adhesive; Dentin; Composite; Adaptation; Tooth; Optical Coherence Tomography; Gap

Introduction

Today, one of the most important advances in clinical dentistry is tooth-colored direct resin restorations [1,2]. Resin composites are continuously developed in attempt to improve its shade, adaptation and bond strength to enamel and dentin [3]. Despite the great advantages of its use, the gap between the composite and the tooth structure created after polymerization is a major concern [4,5]. There is a proportional correlation between gap size with potential hypersensitivity, secondary caries and bacterial invasion that could eventually result in composite failure. Moreover, if these gaps occurred at or below gingival level, they might trap plaque and calculus that would require additional care and management [6,7]. Additionally, interfacial gap formation at the composite margins could be related to the polymerization shrinkage and configuration factor (C-factor) or poor manipulation of the material [8].

Bonding composite restoration to enamel and dentin is technique sensitive, however, bonding to the anisotropic dentin is more complicated that requires considerable attention. Introduction of self-etch adhesive system was a significant advancement in dentistry with simplified bonding technique to dentin and less technique sensitivity due to the absence of acid etching and water-rinsing steps [9-11]. Self-etch adhesives are categorized into two-step and one-step self-etch adhesive systems. Both adhesive systems consist of acidic primers and bonding adhesive. In two-step self-etch adhesive, the primer and bonding are in separate bottles, while they are combined in a single bottle in one-step adhesive [12]. It is worth mentioning that the etching effect of self-etch adhesives is related to the acidic functional monomers that interact with the mineral component of tooth substrate [13]. Literature suggested that adhesive systems might have a direct influence on composite adaptation during cavity restoration [14-16].

There are several testing methods that had been introduced to assess composite adaptation and gap formation at tooth-resin interface [1]. Conventional methods such as tactile probes and x-rays have limitations in evaluating early failure and accurately monitoring a suboptimal marginal interface [17]. Scanning and transmission electron microscopes are other enabled examination tools for detecting the tooth-resin interface at submicron scale, however, these methods are invasive with possibility of error introduced during complicated sample preparation, cross-sectioning and high vacuum processing of the cross-sectioned specimens [18]. Cone-beam computed tomography and computed tomography are non-invasive imaging methods. Yet, the high radiation dose limits their applications and the thick bonding layer could be misinterpreted as recurrent caries. Recently, optical coherence tomography (OCT) is one of the established testing methods to evaluate the adaptation of composite material [19].

OCT has been introduced in dentistry as a non-invasive cross-sectional imaging technique. It uses low-coherence interferometry to produce a two-dimensional image of optical scattering from internal tissue microstructures that is analogous to ultrasonic pulse-echo imaging. It has longitudinal and lateral spatial resolutions of a few micrometers [20]. In microleakage studies, OCT is more conservative with higher accuracy approach compared to dye penetration test and ground sectioning technique [1]. OCT has been effectively utilized to image dental caries, biofilms and biomaterials interaction with dental tissues [21-27]. Moreover, OCT could provide reliable information on the effectiveness and performance of dental composites restoration in quantitative assessment research. Additionally, dental literature concluded that swept-source OCT (SS-OCT) was effectively and non-invasively utilized in determining resin coating integrity and measuring gaps under composite restorations. However, monitoring enamel changes was limited with this system due to formation of the specular reflection at the external tooth surface [28-31].

Although cross-polarization OCT (CP-OCT) was introduced as an alternative system by adding a second polarizer to eliminate the formed specular reflection, very few studies discussed the ability of this system in measuring composite adaptation.

Aim of the Study

The aim of this study was to optically assess the adaptation of two different adhesive systems bonded to two resin composite materials using CP-OCT. The null hypothesis was that there is no difference between the tested adhesive systems in term of their adaptation to class I cavity walls.

Materials and Methods

Materials used

In this vitro study, two resin-based dental adhesive materials; Clearfil SE bond 2, a two-step, self-etch, light-cure bonding adhesive system (SE; Kuraray Noritake Dental, Japan) and Bond Force (Palfique Bond) a one-step, self-etch, light-cure bonding system (PL; Tokuyama Dental, Japan) were used along with two resin-based dental restorative materials; Herculite XRV microhybrid dental composite (HRV; Kerr, Italy) and Estelite alpha composite (ESA; Tokuyama Dental, Japan). The materials used are listed in table 1.

Material (Manufacture) Lot No.	Code	Composition	Fillers volume (Vol%) Fillers Size
Clearfil SE bond 2 Two-step Self-etch Bond (Kuraray Noritake) 5L0010	SE	Primer: <ul style="list-style-type: none"> • 10-MDP • Water • HEMA • Hydrophilic Dimethacrylate • CQ • N, N-Diethanol p-toluidine Bond: <ul style="list-style-type: none"> • Bis-GMA • HEMA • 10-MDP • Hydrophobic Aliphatic Dimethacrylate • Colloidal silica • DI-Camphorquinone • Initiators • Accelerators • N, N- Diethanol p-toluidine 	-
Bond Force (Palfique bond) One-step Self-etch Bond (Tokuyama Dental) 028E26	PL	<ul style="list-style-type: none"> • 3D-SR • HEMA • Bis-GMA • TEGDMA • Glass fillers • Photoinitiators • Isopropyl alcohol • Water • Sodium Fluoride 	-
Herculite XRV Composite (Kerr) 5162588	HRV	<ul style="list-style-type: none"> • Methacrylate Ester Monomers • 7,7,9(or 7,9,9)-trimethyl-4, 13-dioxo-3,14-dioxo-5, 12-diazahexadecane-1, 16-diyl bis-methacrylate • 1,6-hexanediyl bismethacrylate • 2,2'-ethylenedioxydiethyl dimethacrylate • hexamethylene diacrylate • 3-trimethoxysilylpropyl methacrylate • Inert mineral fillers • Activators and stabilizers • Inorganic filler 	<ul style="list-style-type: none"> • (59%) • 0.6 µm
Estelite Alpha Composite (Tokuyama Dental) E6514	ESA	<ul style="list-style-type: none"> • Bis-GMA • Triethylene glycol dimethacrylate • Silica-zirconia spherical filler • Composite filler 	<ul style="list-style-type: none"> • (71%) • 0.2 µm

Table 1: List of the composition of the used adhesives and composites in this study.

Abbreviation: HEMA: 2-Hydroxyethyl Methacrylate; Bis-GMA: Bisphenol A Diglycidyl methacrylate; 10-MDP: 10-Methacryloyloxydecyl dihydrogen phosphate; CQ: Camphorquinone; 3D-SR: Methacryloyloxyalkyl acid phosphate; TEGDMA: Triethyleneglycol dimethacrylate.

Teeth specimen, cavity preparation, and restoration

In this experiment, the collection and usage of the extracted human teeth were subjected to the guidelines of the Ethical Committee of King Abdulaziz University, that are in accordance with principles of Declaration of Helsinki. A Total of 40 non-carious extracted human premolar teeth were collected and visually examined for any soft tissue remnant followed by scaling to clean all the teeth. Reduction of the coronal cusps of each specimen by a high-speed diamond bur to obtain a flat enamel occlusal surface. After that, root trimming was done using a model trimmer for all teeth. Then, cylindrical class-I cavity preparation was prepared on the occlusal surface (1.5 mm in depth × 4 mm in diameter) using wheel diamond bur. After cavity preparation, the specimens were divided randomly into four groups. Each group (n = 10) was bonded with one of the adhesive materials (SE, PL) and light-cured according to the manufacturer instructions. Then, one of the resin composite materials (HRV, ESA) was used to restore the prepared cavities in a bulk filling technique and light-cured according to the manufacturer’s recommendations using LED light cure (1200 mW/cm²). Finally, the specimen was embedded in self-cure epoxy resin except the occlusal surface and coated all around with a double layer of polish varnish, away from the tooth-composite margins by 0.5 mm. Schematic illustration for the methodology is shown in figure 1.

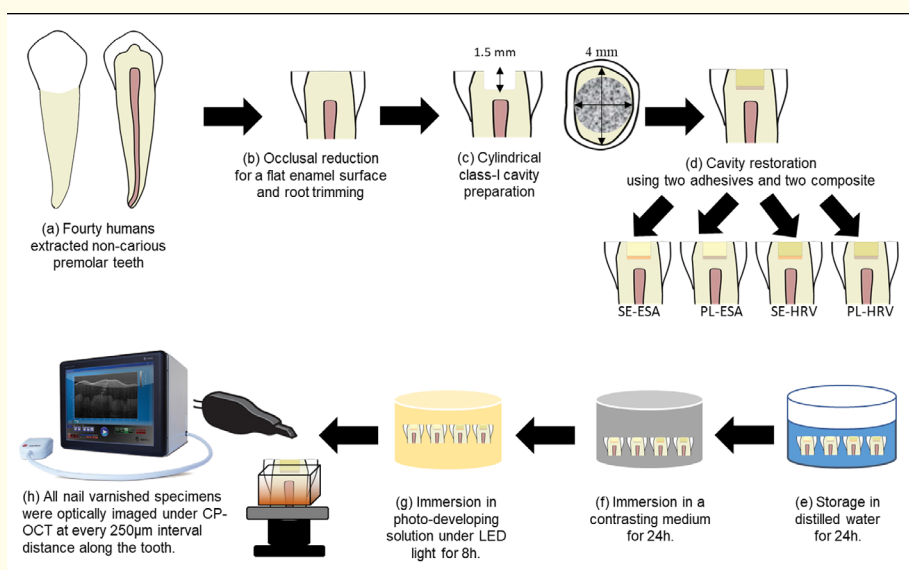


Figure 1: A Schematic illustration that shows the methodology of the study.

Contrasting solution preparation

In this study, Ammoniacal silver nitrate solution is used as a contrasting agent, and the protocol of its preparation was carried out as described in previous study [14]. In a dark room, 25 mg of silver nitrate crystals (Sigma Chemical, USA) were dissolved in 25 ml of distilled water. After that, ammonium hydroxide (28%) (Sigma Chemical, USA) was added to titrate the black, dark solution until it turned to clear and transparent agent.

The varnished specimens were stored in distilled water for 24h. Then, all the specimens were submerged in the silver nitrate solution for 24h, followed by 8h in photo-developing solution under fluorescent light to convert the silver-diamine ions into metallic silver particles. Before OCT imaging, all specimens were washed under distilled water for 30s.

CP-OCT system and data acquisition

The used portable CP-OCT (IVS-300, Santec, Japan) consist of a PC, monitor, 2-axis MEMS scanner and a handheld long neck type probe. This system emits diode laser with high scanning rate (30 kHz) and continuous wavelength centered near 1310 nm, with a wavelength range 100 nm. The axial resolution was around 12 μm with system sensitivity setting of ≥ 95 dB. The probe output power was ≤ 10 mW, which is within the safety limits defined by American National Standard Institute as specified by the manufacturer [32]. The technical specification of the used CP-OCT system is described in table 2. Each specimen was placed perpendicular (90°) to the projected light on a micrometer stage with a standardized fixed distance of 0.25 - 0.5 mm from the laser probe. Serial tomographic B-scan images were taken by CP-OCT for cavity floor assessment at every 250 μm in mesio-distal direction (Figure 1) [19,32].

Cross-Polarization OCT (CP-OCT; IVS-300, Santec, Japan)	
Parameter	Specification
Center Wavelength	1330 ± 30 nm
Scan rate	30 ± 0.1 kHz
Axial resolution	12 μm (in air)
Lateral resolution	= Spot size
System sensitivity	> 95dB
Lateral scan area	≥ 5×5 mm
Imaging depth	3 mm (in air)
Maximum Output Power	≤ 10 mW (Near-infrared Class 1 Laser)

Table 2: Technical specifications of the CP-OCT system.

CP-OCT image analysis

In order to standardize the data acquisition, image processing and gap measurement, each step was performed by the same operator for all groups. The obtained OCT data were reconstructed into a grayscale image using a plug-in macro-file installed into an image analysis software (ImageJ 1.5m9, National Institutes of Health, USA). The reconstructed B-scans were showing the interfacial areas with either a backscattered reflection in the form of a bright white cluster or dark cluster of pixels that represent “gap” or “no gap” respectively, as reported in previous study [14].

The mechanism of OCT imaging and data acquisition and processing and analysis is described in other studies (Figures 2 and 3) [19,32].

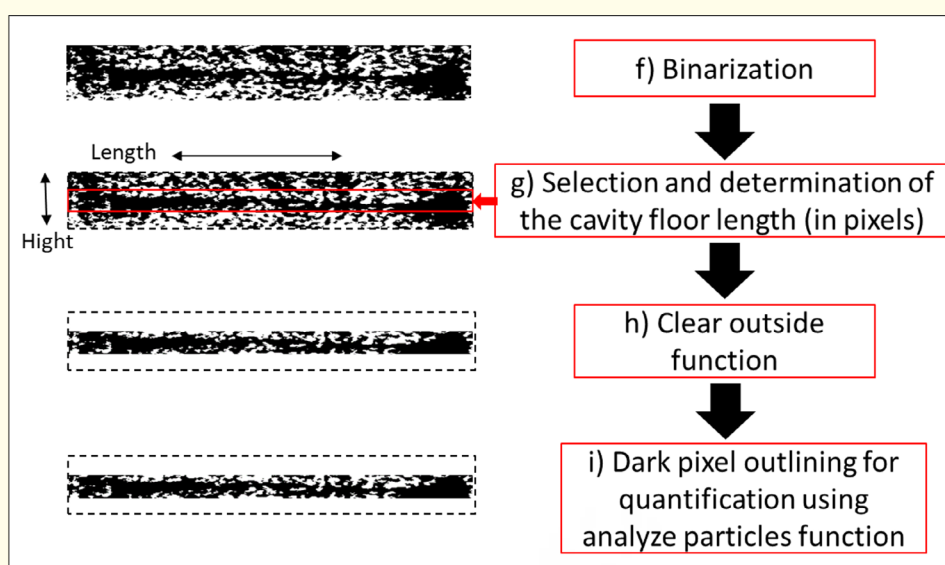


Figure 2: A schematic illustration that shows the steps of image processing during image analysis.

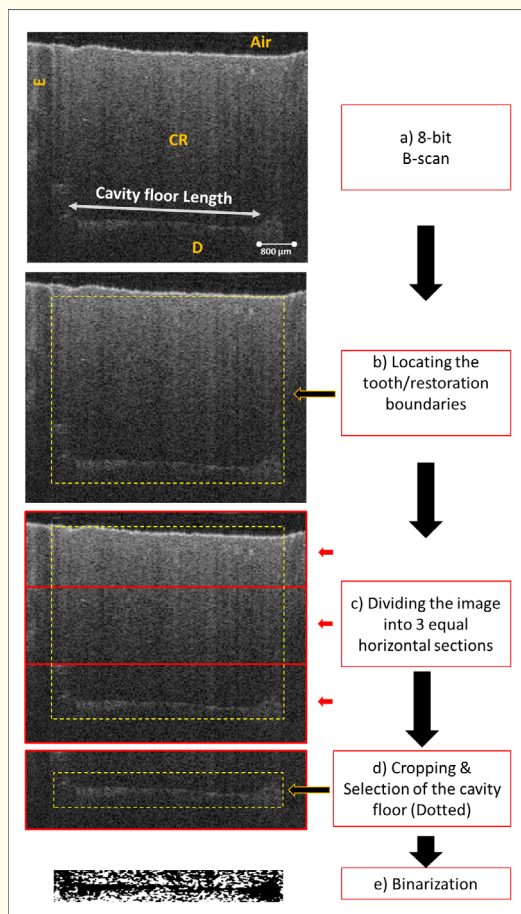


Figure 3: A schematic illustration that shows the steps of image processing for gap quantification.

The analysis and quantification were performed in several steps as follow; the raw OCT data was opened using the macros-function to reconstruct the B-scan image. The size of B-scan was 500×925 pixels corresponding to 5×8.18 mm (x, z). Then, the type of the reconstructed image was set to 8-bit followed by median filter application (1px radius) to the image to minimize the noise. The median filter is a non-linear digital filtering method that is used to eliminate noise as a typical pre-processing. After that, the filtered image was divided into 3 equal horizontal sections. Then, the cavity floor section was cropped followed by determination of the area of interest including the cavity floor in the center, of which the height was 0.5 mm (optical) and the width was equal to that of the cavity floor according to the location of the slice. Then, the binarization process was applied to the cropped image of the cavity floor according to the Isodata algorithm in the auto-threshold function of the software to allocate the target pixels with significantly higher brightness compared to other pixels in the background [33]. In an automated binarization process, the target image is based on a threshold determined automatically using an algorithm. The automated binarization changes a grayscale image to a binary image (bi-level or black and white image), using specific threshold (cut-off range) to visualize important information in an image. On the binary image, the length of cavity floor was selected, and clear-outside function was employed to remove the unnecessary pixels around the tooth-restoration interface. Then, the cavity floor was measured (in pixels) and each dark cluster of pixels on the white background was carefully selected using rectangular selection and

calculated using analyze particle function. After that, dark cluster length percentage (gap %) of the cavity floor on each cross-section was calculated according to the following equation:

$$Gap\ Percentage = \frac{Gap\ length}{Total\ floor\ length} \times 100$$

Statistical analysis

Data normality was assessed using Shapiro-Wilk test, and it was statistically significant (p = 0.00). This finding indicated a non-normal distributed data, therefore non-parametric analyses were utilized. Kruskal-Wallis test was conducted to determine if there were differences in median gap percentages among the tested adhesives. Subsequently, pairwise comparisons were performed using Mann-Whitney test.

Results

The obtained results in this study are presented in figures 4-7. Upon inspecting the obtained B-scan images, some images showed strong signal intensity at the tooth-resin interface. Some areas demonstrated a bright white cluster of pixels, which indicated poor composite adaptation and gap formation at the bonded interface. On the hand, other areas showed low signal intensity that are devoid of bright clusters and represent acceptable adaptation with no gap or loss of interfacial seal. By analyzing the obtained data (Figure 8), it showed a significant difference between all the groups except between SE-ESA and PL-ESA (p = 0.51). The highest median gap percentage was seen in PL-HRV group followed by SE-ESA, PL-ESA and SE-HRV, respectively (Table 3).

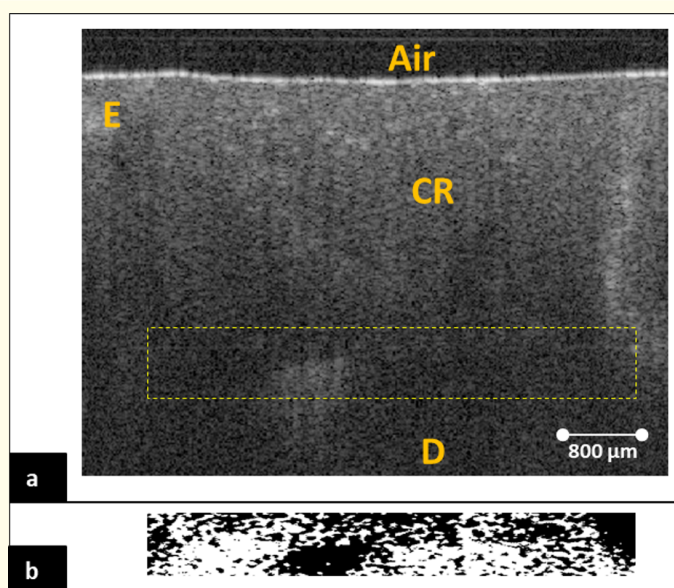


Figure 4: Representative B-scan for SE-ESA group in (a). Image (b) is a binary image for the dotted box in (a) at the cavity floor. The center of the cavity floor in (a) is showing high signal intensity in the form of bright pixels that was corresponding to the dark pixels in (b). CR: Composite resin, E: Enamel, D: Dentin.

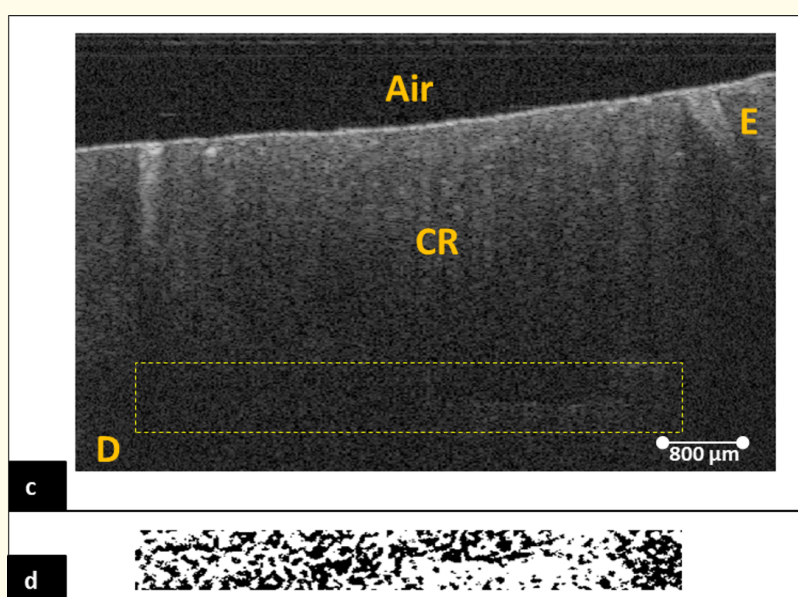


Figure 5: Representative B-scan for PL-ESA group in (c). Image (d) is a binary image for the dotted box in (c) at the cavity floor. The cavity floor in (c) showed high signal intensity in the form of bright pixels at the right side of the cavity floor and which was corresponding to the dark pixels in (d). CR: Composite resin, E: Enamel, D: Dentin.

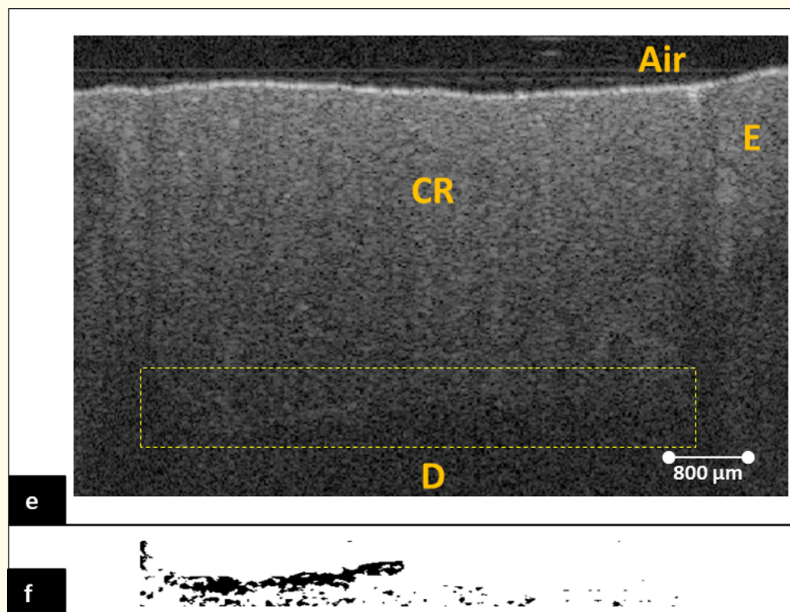


Figure 6: Representative B-scan for SE-HRV group in (e). Image (f) is a binary image for the dotted box in (e) at the cavity floor. The cavity floor in (e) showed high signal intensity in the form of bright pixels at the left side of the cavity that was corresponding to the continuous band of dark pixels in (f). CR: Composite resin, E: Enamel, D: Dentin.

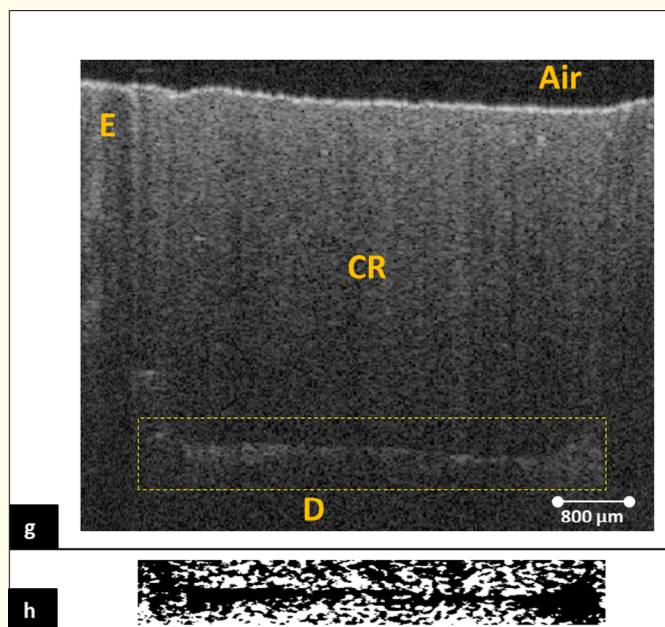


Figure 7: Representative B-scan for PL-HRV group in (g). Image (h) is a binary image for the dotted box in (g) at the cavity floor. The cavity floor in (g) showed high signal intensity in the form of continues band of bright pixels that were corresponding to the dark pixels in (h). CR: Composite resin, E: Enamel, D: Dentin.

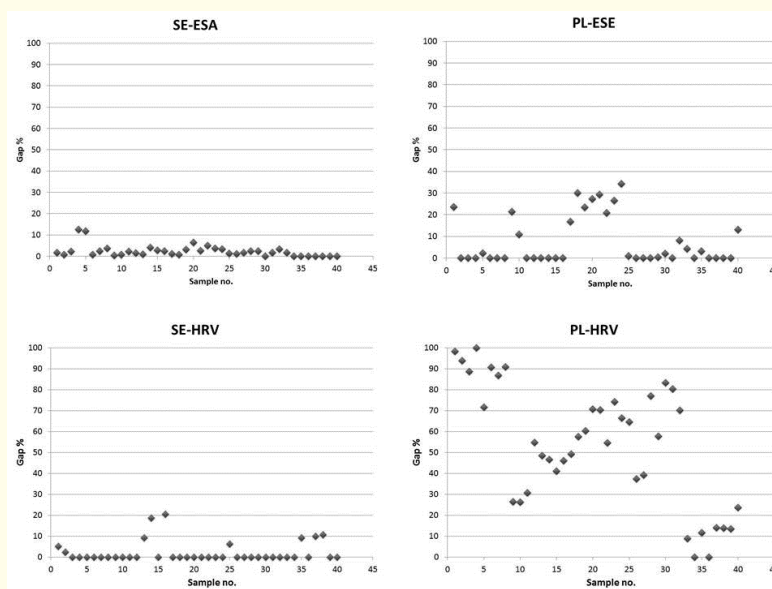


Figure 8: The scatter plot of the specimens in each group. It showed a significant difference between all the groups except between SE-ESA and PL-ESA with the highest median gap % was seen in PL-HRV group followed by SE-ESA, PL-ESA and SE-HRV.

Group	Gap percentage (%)		
	Mean% (\pm SD)	Median% (25 th -75 th percentile)	Mean rank
SE-ESA	2.3 (2.8)	1.62 (0.68 - 2.98) ^a	72.74
PL-ESA	7.44 (11.1)	0 (0 - 14.86) ^a	67.56
SE-HRV	2.29 (5.1)	0 (0) ^b	47.88
PL-HRV	53.47 (29.1)	56.15 (28.57 - 75.52) ^c	133.83

Table 3: Gap percentage values of the tested groups.

The different superscripts indicate statistically significant differences between groups.

Discussion

The performance of the tested adhesive restorations was evaluated in term of cavity adaptation. SE-HRV showed the best cavity adaptation with the lowest gap detected, compared to other tested groups. Thus, the null hypothesis was rejected.

It is known that poor oral hygiene in the presence of cariogenic bacteria could lead to destruction of tooth substance that would require restoration of the damaged part. Nowadays, MI concept or so-called “minimum intervention” is the current trend in dentistry. Generally, adhesive restorations falls under this concept [34]. Dental composites are widely used as tooth-colored restoration because it satisfies patient cosmetic demand as well as conservative as it relies on the adhesiveness of the resin rather than cavity geometry [35]. However, de-bonding due to either water sorption or the release of bacterial esterase and bonding hydrolysis could result in gap formation that would promote bacterial accumulation and recurrent caries formation, which might end up with failure of the restoration [18,36,37].

Many studies investigated gap formation under composite using compressed air, dye penetration, bacteria and radioactive markers [38,39]. However, these methods are either invasive or require prolonged time for acquisition and processing. Both ultrasounds and micro-CT are non-destructive imaging techniques utilized to assess composite adaptation and gap formation, yet, the lower resolution in the former and high radiation dosage in the latter was a major drawback. Moreover, current OCT systems showed superior images and

results compared to other methods [19,20,40]. CP-OCT system differs from SS-OCT in including a second polarizer to remove the mirror-like reflection. This setup made CP-OCT system a useful tool for demineralization and remineralization studies. To broaden the application of CP-OCT in adaptation studies, specimens were immersed in metallic contrasting agent to intensify the gap appearance and to improve the gap reflection under the composite restoration [16]. Ammoniacal silver-nitrate solution had been widely employed in nanoleakage studies. The silver ions in the solution can easily penetrate the interfacial spaces and transform into silver grains upon light exposure [16,24]. Upon CP-OCT imaging, areas with heavy accumulation of silver had scattered the light into different direction and produced diffuse reflections (bright pixels). While the areas that are devoid of silver particles were not showing any considerable reflection in a form of bright pixels [16].

Median filtering is generally less sensitive to outliers than mean filtering. In this study, the 1px radius was selected in median filtering to reduce the noise that would be seen in B-scans without reducing the image quality or producing a blurring effect [41].

It is known that a gradual loss of signal intensity is anticipated in some areas as the light travels through the composite and deep into dentin layer. If the refractive index of enamel, dentin and composite are in the range $n = 1.5 - 1.6$ were assumed, then light intensity would be consumed during its passage [19,42]. This finding could be considered as one explanation for the poor morphological appearance of the dentin seen in figure 5 and 6. Another explanation would be related to the contrasting agent used to overcome the difficulty in gap imaging. The contrasting agent used in the current study facilitated gap detection under the restoration, however it could adversely affect the imaging of the underlying dentin as seen in figure 7.

C-factor is defined as the ratio of bonded to unbonded surface area of a restoration [43]. It is considered an influencing factor on composite adaptation against contraction stresses. Many studies showed a positive correlation between gap formation and the C-factor [44]. In this study, the highest gap percentage was seen in PL-HRV group followed by SE-ESA, PL-ESA, SE-HRV, respectively. The last three groups; SE-ESA, PL-ESA, SE-HRV, showed less than 10% of gap. This indicated a strong adaptation and high adhesive performance correspondingly. The results of this study suggest that gap formation is a multifactorial defect that not only related to C-factor, but also related to the type of composite and adhesive system.

SE adhesive is a two-step self-etch adhesive system containing Methacryloyloxydecyl dihydrogen phosphate (MDP) monomer, which has a high binding affinity to hydroxyapatite [44]. Nurrohman, *et al.* reported that the acidic functional monomers of MDP-based self-etch adhesives used on dentin might cause incomplete demineralization of the apatite to form a strong chemical bond with an acid-base resistant zone (ABRZ) beneath the hybrid layer [45]. Additionally, bond strength and durability studies suggested superior performance of MDP-based adhesive [46]. On the other hand, the volume of fillers in HRV and ESA composites are around 59% and 71%, respectively. In this study, the adaptation of SE-ESA group was significantly lower than SE-HRV group. Unlike HRV composite, the high filler loading in ESA composite are expected to reduce the polymerization shrinkage. However, this high filler loading had raised the contraction stresses in high C-factor cavity design, which adversely affected the composite adaptation and explain the present results of these two groups.

PL adhesives is a fluoride-containing adhesive that contains 3D-SR functional monomer. The strong bond created by the 3D-SR functional monomer contribute to the adhesive bond longevity [47]. Moreover, the fluoride content in this adhesive would be responsible for the creation of ABRZ [48].

It is known that the weakest point in any restoration is the adhesive interface. The results of this study showed an improved adaptation of PL-ESA group, where both the composite and the bonding resin were from the same manufacturer. This finding is supported by a report that showed a significant increase in the bond strength when the composite was repaired with a composite from the same manufacturer [49]. Compatibility between the co-polymers of the bonded materials might be a possible explanation of the obtained results in PL-ESA in comparison to PL-HRV. Although many reports presented the superior performance of two-step self-etch adhesives over one-step

[16,50,51], the obtained results showed no significant difference between SE-ESA and PL-ESA groups. It seems that the co-polymer compatibility between the bonded resins in PL-ESA had played a significant role in improving the PL performance and gap reduction under the composite. On the contrary, the mismatch between the co-polymers in PL-HRV could explain the lower performance in this group.

Conclusions

Within the limitations of this *in vitro* study, it can be concluded that gap beneath a composite can be assessed non-destructively by using CP-OCT. Other than composite filler loading and adhesive formula, the interactions of the adhesive and composite co-polymers have great influence on composite adaptation. Ammoniacal silver-nitrate medium has a great potential in OCT microleakage studies by signaling the gap with bright pixels.

Acknowledgment

This study was supported by Faculty of Dentistry, King Abdulaziz University, Jeddah, Saudi Arabia.

Conflicts of Interest

The authors declare no conflict of interest.

Bibliography

1. Bakhsh TA, *et al.* "Relationship between non-destructive OCT evaluation of resins composites and bond strength in a cavity". Proceedings of BiOS Photonic West SPIE, Lasers in Dentistry XVIII, USA, Peter Rechmann, Daniel Fried SPIE: San Francisco, USA (2012): 8208.
2. Liang Y, *et al.* "Micro-invasive interventions for managing non-cavitated proximal caries of different depths: a systematic review and meta-analysis". *Clinical Oral Investigations* 22.8 (2018): 2675-2684.
3. Van Landuyt KL, *et al.* "Systematic review of the chemical composition of contemporary dental adhesives". *Biomaterials* 28.26 (2007): 3757-3785.
4. Estafan D and Agosta C. "Eliminating microleakage from the composite resin system". *General Dentistry* 51.6 (2003): 506-509.
5. Bagis YH, *et al.* "Comparing microleakage and the layering methods of silorane-based resin composite in wide Class II MOD cavities". *Operative Dentistry* 34.5 (2009): 578-585.
6. Isola G, *et al.* "The effects of a desiccant agent in the treatment of chronic periodontitis: a randomized, controlled clinical trial". *Clinical Oral Investigations* 22.2 (2018): 791-800.
7. Matarese G, *et al.* "The Effects of Diode Laser Therapy as an Adjunct to Scaling and Root Planing in the Treatment of Aggressive Periodontitis: A 1-Year Randomized Controlled Clinical Trial". *Photomedicine and Laser Surgery* 35.12 (2017): 702-709.
8. Sadr A, *et al.* "Swept source optical coherence tomography for quantitative and qualitative assessment of dental composite restorations". Proceedings of BiOS Photonic West SPIE, Lasers in Dentistry XVII, USA, Peter Rechmann, Daniel Fried SPIE: San Francisco, USA (2011).
9. Bakhsh TA, *et al.* "In situ characterization of resin-dentin interfaces using conventional vs. cryofocused ion-beam milling". *Dental Materials* 31.7 (2015): 833-844.
10. Marghalani HY, *et al.* "Ultramorphological assessment of dentin-resin interface after use of simplified adhesives". *Operative Dentistry* 40.1 (2015): E28-E39.

11. Marghalani HY, *et al.* "Ultra-structural characterization of enamel-resin interface using FIB-TEM technology". *Journal of Adhesion Science and Technology* 28.11 (2014): 1005-1019.
12. Van Meerbeek B, *et al.* "State of the art of self-etch adhesives". *Dental Materials* 27.1 (2011): 17-28.
13. Yazici AR, *et al.* "Bond strength of one-step self-etch adhesives and their predecessors to ground versus unground enamel". *European Journal of Dentistry* 6.3 (2012): 280-286.
14. Turkistani A, *et al.* "Optical Evaluation of Enamel Microleakage with One-Step Self-Etch Adhesives". *Photomedicine and Laser Surgery* 36.11 (2018): 589-594.
15. Bakhsh TA, *et al.* "Optical Quantification of Microgaps at Dentin-Composite Interface". *Biomedical Physics and Engineering Express* 4.4 (2018): 045030.
16. Bakhsh TA, *et al.* "Effect of self-etch adhesives on the internal adaptation of composite restoration: a CP-OCT Study". *Odontology* 107.2 (2018): 165-173.
17. Lammeier C, *et al.* "Influence of dental resin material composition on cross-polarization-optical coherence tomography imaging". *Journal of Biomedical Optics* 17.10 (2012): 106002.
18. Ikeda I, *et al.* "Effect of filler content of flowable composites on resin-cavity interface". *Dental Materials Journal* 28.6 (2009): 679-685.
19. Bakhsh TA, *et al.* "Non-invasive quantification of resin-dentin interfacial gaps using optical coherence tomography: validation against confocal microscopy". *Dental Material* 27.9 (2011): 915-925.
20. Huang D, *et al.* "Optical coherence tomography". *Science* 254.5035 (1991): 1178-1181.
21. Lenton P, *et al.* "Imaging in vivo secondary caries and ex vivo dental biofilms using cross-polarization optical coherence tomography". *Dental Material* 28.7 (2012): 792-800.
22. Rasmussen K, *et al.* "Real-time imaging of anti-biofilm effects using CP-OCT". *Biotechnology and Bioengineering* 113.1 (2016): 198-205.
23. Shimada Y, *et al.* "Validation of swept-source optical coherence tomography (SS-OCT) for the diagnosis of occlusal caries". *Journal of Dentistry* 38.8 (2010): 655-665.
24. Makishi P, *et al.* "Non-destructive 3D imaging of composite restorations using optical coherence tomography: Marginal adaptation of self-etch adhesives". *Journal of Dentistry* 39.4 (2011): 316-325.
25. Chan KH and Fried D. "Multispectral cross-polarization reflectance measurements suggest high contrast of demineralization on tooth surfaces at wavelengths beyond 1300 nm due to reduced light scattering in sound enamel". *Journal of Biomedical Optics* 23.6 (2018): 1-4.
26. Jang AT, *et al.* "Automated ablation of dental composite using an IR pulsed laser coupled to a plume emission spectral feedback system". *Lasers in Surgery and Medicine* 49.7 (2017): 658-665.
27. Wijesinghe RE, *et al.* "Bio-Photonic Detection and Quantitative Evaluation Method for the Progression of Dental Caries Using Optical Frequency-Domain Imaging Method". *Sensors (Basel)* 16.12 (2016): E2076.
28. Alsayed EZ, *et al.* "Optical coherence tomography for evaluation of enamel and protective coatings". *Dental Materials Journal* 34.1 (2015): 98-107.

29. Schneider H., *et al.* "Dental Applications of Optical Coherence Tomography (OCT) in Cariology". *Applied Sciences* 7.5 (2017): 472.
30. Mandurah MM., *et al.* "Monitoring remineralization of enamel subsurface lesions by optical coherence tomography". *Journal of Biomedical Optics* 18.4 (2013): 046006.
31. Natsume Y., *et al.* "Estimation of lesion progress in artificial root caries by swept source optical coherence tomography in comparison to transverse microradiography". *Journal of Biomedical Optics* 16.7 (2011): 071408.
32. Bakhsh TA., *et al.* "Novel evaluation and treatment techniques for white spot lesions. An in vitro study". *Orthodontics and Craniofacial Research* 20.3 (2017): 170-176.
33. "Picture Thresholding Using an Iterative Selection Method". *IEEE Transactions on Systems, Man, and Cybernetics* 8.8 (1978): 630-632.
34. Dawson AS and Makinson OF. "Dental treatment and dental health. Part 1. A review of studies in support of a philosophy of Minimum Intervention Dentistry". *Australian Dental Journal* 37.2 (1992): 126-132.
35. Mikulas K., *et al.* "[Paradigm shift in conservative dentistry: the end of the amalgam era]". *Orvosi Hetilap* 159.42 (2018): 1700-1709.
36. Pinna R., *et al.* "The role of adhesive materials and oral biofilm in the failure of adhesive resin restorations". *American Journal of Dentistry* 30.5 (2017): 285-292.
37. Huang B., *et al.* "Esterase from a cariogenic bacterium hydrolyzes dental resins". *Acta Biomaterialia* 71 (2018): 330-338.
38. Alani AH and Toh CG. "Detection of microleakage around dental restorations: a review". *Operative Dentistry* 22.4 (1997): 173-185.
39. de Santi Alvarenga FA., *et al.* "Reliability of marginal microleakage assessment by visual and digital methods". *European Journal of Dentistry* 9.1 (2015): 1-5.
40. Fujimoto JG., *et al.* "Optical coherence tomography: an emerging technology for biomedical imaging and optical biopsy". *Neoplasia* 2.1-2 (2000): 9-25.
41. Abdessamad Ben Hamza., *et al.* "Removing Noise and Preserving Details with Relaxed Median Filters". *Journal of Mathematical Imaging and Vision* 11.2 (1999): 161-177.
42. Hariri I., *et al.* "Effects of structural orientation of enamel and dentine on light attenuation and local refractive index: an optical coherence tomography study". *Journal of Dentistry* 40.5 (2012): 387-396.
43. Feilzer AJ., *et al.* "Setting stress in composite resin in relation to configuration of the restoration". *Journal of Dental Research* 66.11 (1987): 1636-1639.
44. dos Santos GO., *et al.* "Analysis of gap formation at tooth-composite resin interface: effect of C-factor and light-curing protocol". *Journal of Applied Oral Science* 15.4 (2007): 270-274.
45. Nurrohman H., *et al.* "Apatite crystal protection against acid-attack beneath resin-dentin interface with four adhesives: TEM and crystallography evidence". *Dental Materials* 28.7 (2012): e89-e98.
46. Inoue S., *et al.* "Hydrolytic stability of self-etch adhesives bonded to dentin". *Journal of Dental Research* 84.12 (2005): 1160-1164.
47. Yoshida Y., *et al.* "X-ray diffraction analysis of three-dimensional self-reinforcing monomer and its chemical interaction with tooth and hydroxyapatite". *Dental Materials Journal* 31.4 (2012): 697-702.
48. Tsujimoto M., *et al.* "Ultrastructural observation of the acid-base resistant zone of all-in-one adhesives using three different acid-base challenges". *Dental Materials Journal* 29.6 (2010): 655-660.

49. Forsten L and Valiaho ML. "Transverse and bond strength of restorative resins". *Acta Odontologica Scandinavica* 29.5 (1971): 527-537.
50. Ishikawa A., *et al.* "Micro-tensile and micro-shear bond strengths of current self-etch adhesives to enamel and dentin". *American Journal of Dentistry* 20.3 (2007): 161-166.
51. Yuan Y., *et al.* "Effects of dentin characteristics on interfacial nanoleakage". *Journal of Dental Research* 86.10 (2007): 1001-1006.

Volume 18 Issue 6 June 2019

©All rights reserved by Turki A Bakhsh., *et al.*